Vol. A52 (1977) *ACTA PHYSICA POLONICA* No 5

A STUDY OF QUASI-ELASTIC NEUTRON SCATTERING IN PHASE II OF t-NITROBUTANE

By J. Mayer, I. Natkaniec, J. Ściesiński

Institute of Nuclear Physics, Cracow*

and S. Urban

Institute of Physics of the Jagellonian University, Cracow**

(Received March 21, 1977)

The results of quasi-elastic neutron scattering (QNS) investigations are presented for phases II and III of t-nitrobutane (TBN, $(CH_3)_3CNO_2$) in the range of momentum transfers from 0.96 to 2.56 $Å^{-1}$. The neutron spectra obtained for phase III correspond to the spectrometer resolution function, whereas in phase II distinct quasi-elastic broadening is observed. Two models of uniaxial reorientational motion of protons were considered in the QNS pattern analysis, namely, proton jumps by an angle of 120° around the C—C axis (CH_3 group rotation) and rotations of molecules around the C—N axis. The latter involved two extremes of molecular reorientation: jumps by 120° and rotational diffusion. It was ascertained that in TBN phase II there exists a stochastic uniaxial reorientation of molecules with a correlation time of about 1.6×10^{-12} sec, and the model of 120° jumps is given preference.

1. Introduction

The quasi-elastic neutron scattering (QNS) method is an important tool used in research on proton dynamics in molecular systems. In contradistinction to other methods, QNS is sensitive not only to the time parameters of the stochastic proton motion but also to the geometrical parameters of this motion. This is particularly useful when other methods (especially nuclear magnetic resonance) fail due to the enormous rate at which the dynamic processes occur. The greatest weakness of the QNS method is its insufficient energy resolution in most of the currently existing neutron spectrometers. This considerably limits the possibilities of examining the finer effects. Therefore the results acquired are of a qualitative, rather than quantitative, nature. This is also true in the case of the KD SOG-1 inverted-geometry spectrometer installed at the IBR-1 pulsed reactor of the JINR, Dubna,

* Address: Instytut Fizyki Jądrowej, Radzikowskiego 152, 31-342 Kraków, Poland.
** Address: Instytut Fizyki, Uniwersytet Jagielloński, Reymonta 4, 30-059 Kraków, Poland.

on which the present investigation of molecular reorientation in phase II of t-nitrobutane was carried-out.

t-Nitrobutane (TBN, 2-methyl-2-nitropropane) belongs to the group of compounds of the general chemical formula $(CH_3)_3CX$ (X = Cl, Br, NO_2 or CN), the molecules of which feature orientational freedom in the solid phases. TBN, like the other three compounds, exhibits two phase transitions in the solid state which demarcate three phases: phase I between the melting point at 299.2 K and the first phase transition at 260.1 K (ΔS = 4.28 e. u.), phase II between 260.1 K and the second phase transition at 215.3 K (ΔS = 4.69 e. u.), and phase III below 215.3 K [1]. The structure of phase I is orthorhombic. Phase II has triclinic symmetry of the following unit cell parameters: a = 7.19 Å, b = 6.22 Å, c = 7.25 Å, $\alpha = 90°14'$, $\beta = 88°32'$ and $\gamma = 87°40'$ [1]. Dielectric studies of TBN have shown that phase I is a typical rotational phase, in which similarly as in the liquid phase the dipole moments of the molecules perform rotational movements hindered by a low energy barrier (of the order of 1 kcal/mole) [2]. Measurements of the static dielectric constant have shown that in TBN phase II the dipole moments of the molecules do not have orientational freedom, but perform librations of a relatively high amplitude, whence this phase has been named the "librational phase" [3]. Such large librations and relatively loose packing of molecules in the crystal unit cell [4] implied the existence of reorientational motions of the molecules about the C–N axis in phase II. A similar suggestion follows from an analysis of the entropy of the phase II — to — phase III transition [1] and from studies of absorption in the far infrared [5].

QNS measurements performed earlier for a similar compound, t-butyl chloride (TBC, X = Cl in the general formula), revealed that its phase II features uniaxial rotation of molecules around C–Cl axis with a correlation time of the order of 5 psec [6]. Analyses of several rotation models enabled us to give preference to the model embodying jumps of trimethyls by an angle of 120°. Despite the essential difference in the crystal lattice symmetry of phases II of TBN and TBC (TBC is tetragonal with a = 7.08 Å and c = 6.14 Å [7]), the unit cells in the two cases differ only slightly.

Bearing all that in mind, it was decided that QNS measurements should also be performed for TBN's phase II. In the analysis of the QNS spectra two models of proton reorientational movements will be considered: proton jumps by an angle of 120° around the C–C axis (CH_3 group rotation) and rotations of molecules around the C–N axis, where two extreme cases will be examined; viz., jumps by 120° and rotational diffusion.

2. Some remarks on theoretical models

A specific form of incoherent cross section for quasi-elastic neutron scattering is known only for several simple molecule reorientational models [8]. Hitherto, in analysing the results of experiments concerning molecular reorientation in crystalline substances, one-parameter models have mostly been used. The parameter is either the mean time elapsing between jumps of molecules from one potential minimum to another, or the time that is the inverse of the rotational diffusion coefficient of the models assuming a diffusion-wise change of molecular orientation. In those cases the scattering law for uniaxial molec-

ular reorientation and polycrystalline samples can be described as

$$S^{\mathrm{inc}}_{\mathrm{qel}}(\kappa, \omega) \sim \sum_{H}\left[F_{\mathrm{el}}(\kappa r_H)\delta(\omega)+\frac{2}{\pi}\sum_{l=1}^{n}F^{(l)}_{\mathrm{qel}}(\kappa r_H)\frac{\Gamma_l}{\Gamma_l^2+\omega^2}\right], \tag{1}$$

where: $\hbar\kappa = (\hbar k_i - k_f)$ is the momentum transfer ($\kappa^2 = k_i^2 + k_f^2 - 2k_i k_f \cos\vartheta$, ϑ is scattering angle), $\hbar\omega = E_i - E_f$ is the neutron energy transfer, $k[\text{Å}^{-1}] = 2\pi/\lambda = 0.6947\ E(\text{meV})$ is the value of the neutron wave vector (the indices "i" and "f" denote the initial and final values, respectively, of the neutron wave vector and energy), r_H is the rotation radius of a given proton, and Γ_l, being a function of the model's parameter, is the half-width at half height of the Lorentzian curve.

Specific formulae for the elastic scattering form factor $F_{\mathrm{el}}(\kappa r)$ and the quasi-elastic scattering form factor $F_{\mathrm{qel}}(\kappa r)$ are given in Refs [9–11] for the jump-wise models of proton rotation and in Ref. [11] for the rotational diffusion model. The numerical values of those

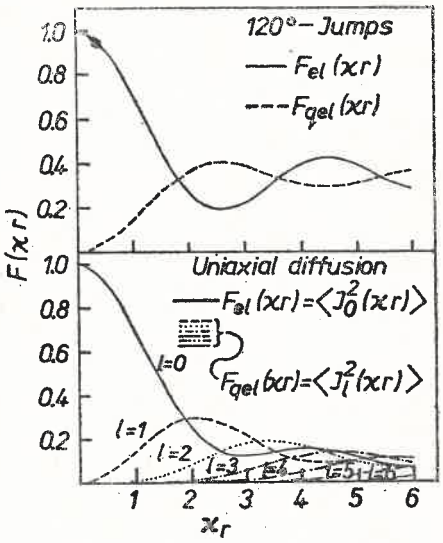

Fig. 1

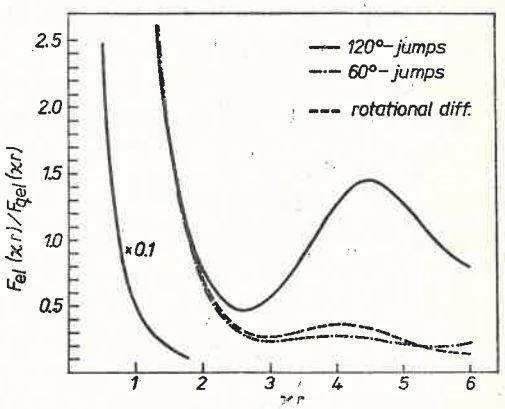

Fig. 2

Fig. 1. Elastic E_{el} and quasi-elastic F_{qel} form factors vs κr for two models of proton rotation
Fig. 2. Ration of the elastic and quasi-elastic form factors for different models of proton rotation

form factors for the models discussed in this study are shown in Fig. 1, while their ratio is presented in Fig. 2.

For 120° proton jumps the quasi-elastic part of the scattering law is represented by one Lorentzian function of half-width $\Gamma = 3\hbar/2\tau$, where τ is the mean time between jumps. On the other hand, in the case of rotational diffusion $S^{\mathrm{inc}}_{\mathrm{qel}}$ is the sum of an infinite series of Lorentz functions of half-width $\Gamma_l = D_r l^2$, where $l = 1, 2, \ldots$, and D_r is the rotational diffusion coefficient. These models are extreme cases of proton reorientation which may occur in the examined crystal. The form factors from Figs 1 and 2 indicate when the models will be distinguishable in the neutron scattering experiment.

For small κr values the elastic scattering form factors are practically identical for the two models; the difference between them becomes distinguishable beginning with $\kappa r > 2$. A comparison of the F_{el}/F_{qel} ratios (Fig. 2) also reveals that the differences between the 120° - jump model and the rotational diffusion model become manifest only when $\kappa r > 2$. The value of this ratio gives an idea of the radius of proton rotation in the sample. Namely, if the two rotation radii differing by, eg. a factor of two are considered (in our case the rotation of the CH_3 groups and the rotation of the molecule), the quasi-elastic broadening should be visible beginning with the smallest values of κ measured in this experiment for molecular rotation, whereas the effect of CH_3 group rotation becomes visible only for larger scattering angles. Attention should be drawn to the fact that the QNS method in the considered κr range is rather insensitive to the intermediate models of proton reorientation for, as shown in Fig. 2, the 60°-jump model is practically the same as the rotational diffusion model.

3. Experimental

The QNS spectra were measured by the time-of-flight technique on an inverted-geometry KD SOG-1 spectrometer at the IBR-1 pulsed reactor of the Neutron Physics Laboratory, JINR, Dubna. The principle of the spectrometers operation is presented in Ref. [12].

The energy of the incident neutrons was analysed by the time-of-flight method over a reactor — sample distance of $L_1 = 30.22$ m, while the scattered neutron energy was determined by a Be-filter — Zn (002) single crystal system. The single crystals were oriented in such a way that their maximum reflectivity was near the Be-filter cut-off ($E_g = 5.24$ meV). The neutrons reflected off the single crystal were detected by a set of ^{3}He counters 180×180 mm^2 in area with an efficiency of about 95%. The mean energy of the neutrons detected after scattering was $\overline{E}_f = 5.06$ meV, while its mean spread at half peak height was $\Delta\overline{E}_f = 0.356$ meV. The energy resolution was therefore about 7%. Spectra for seven scattering angles ϑ 36°, 56°, 76°, 90°, 110°, 130°, and 150° were measured simultaneously.

The TBN sample, identical with the one used in [1], was poured into an aluminium measuring vessel and then quickly solidified. The vessel consisted of two circular plates of 20 cm in diameter screwed together. The sample thickness $d = 0.8$ mm. The vessel was placed in a cryostat [13] and cooled down to the required temperature. The sample temperature was measured by means of three copper-constantan thermocouples, two of which were co-mounted at the edge and one at the center of the vessel. The temperature gradient did not exceed 1.5 K.

4. Experimental results and data processing

The QNS measurements of the TBN sample were carried out at two temperatures corresponding to phase III ($T = 150$ K) and phase II ($T = 240$ K) of the substance. Besides, the background of scattered neutrons was measured with the empty vessel in the cryostat (at room temperature).

Because the Bragg reflections from the substance and aluminium (vessel and cryostat) appear near the energy E_f for large scattering angles, the data analysis which follows will neglect the results obtained for the angles 130° and 150°. The analyzed momentum transfers range between 0.96 $Å^{-1}$ and 2.56 $Å^{-1}$.

The intensity and shape of the quasi-elastic peak (after the vessel and cryostat background is subtracted) in the time-of-flight scale for phases III and II of TBN are shown in Fig. 3. The shape of the peak of phase III corresponds to the resolution function of the

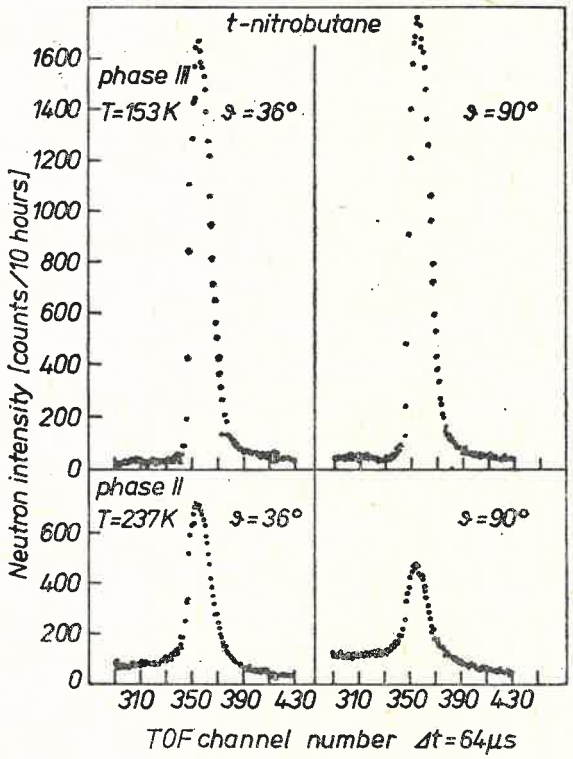

Fig. 3. Neutron spectra measured for TBN's phase II and III in the time-of-flight (TOF) scale

spectrometer measured by analyzing neutrons scattered elastically on vanadium. In phase II the elastic scattering intensity decreases considerably and the peak shape becomes altered, which is evidence that there is quasi-elastic neutron scattering on the sample. There is also a change in the background due to inelastic neutron scattering on the sample, the intensity fraction of which increases with increasing scattering angle.

The neutron intensity in the time-of-flight scale, presented in Fig. 3, can be expressed by formula [12]

$$I(t_0) \sim \Delta t_0 \int dE_i \int dE_f \int dt \varrho(t) \Phi(E_i) \sigma(E_i, E_f, \vartheta, T) R(E_f) \times \delta\left(t_0 - t - \frac{\alpha L_1}{\sqrt{E_i}} - \frac{\alpha L_2}{\sqrt{E_f}}\right), \quad (2)$$

where $\varrho(t)$ is the time distribution and $\Phi(E_i)$ is the energy distribution of the neutrons emerging from the reactor; $R(E_f)$ is the energy distribution of the neutrons recorded after scattering; $\sigma(E_i, E_f, \vartheta, T)$ is the cross section describing the probability of neutron scattering on the sample, and $\delta\left(t_0 - t - \frac{\alpha L_1}{\sqrt{E_i}} - \frac{\alpha L_2}{\sqrt{E_f}}\right)$ is a condition which has to be fulfilled if a neutron leaving the source at time t with energy E_i and scattered on the sample to energy E_f is to be recorded at time t_0 ($\alpha = 2286.2\ \mu s \times meV^{1/2} \times cm^{-1}$ is a factor converting neutron energy into time of flight, $L_2 = 1.42$ m is the mean distance between sample and detector).

Assuming that the $\varrho(t)$ and $R(E_f)$ distributions are narrow enough for the energy of the neutrons incident to the sample to be expressed in terms of their mean values $\bar{t}$ and $\bar{E}_f$ $\left(\text{which may be done in our case because } t_0 \gg t + \frac{\alpha L_2}{\sqrt{E_f}}\right)$, we get

$$\bar{E}_i(t_0) = \frac{\alpha^2 L_1^2}{(t_0 - \bar{t} - \alpha L_2/\sqrt{\bar{E}_f})^2} = E_0. \tag{3}$$

Performing an appropriate exchange of variables and making use of the properties of the δ-function, we can present the intensity of scattered neutrons in the incident neutron energy E_0 scale in the form

$$I(E_0) = \frac{I(t_0)}{\Phi(t_0)} = \text{const} \times \int \sigma(E_0, E_f, \vartheta, T) R(E_f) dE_f, \tag{4}$$

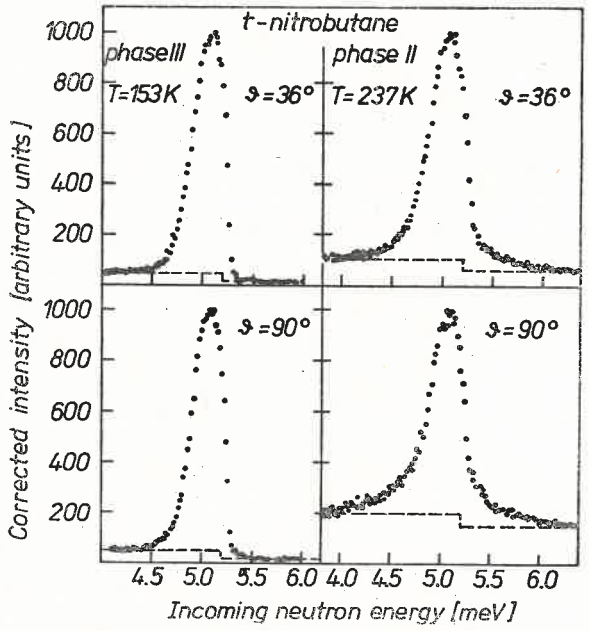

Fig. 4. Normalized neutron spectra presented in Fig. 3 vs incoming neutron energy scale (dashed lines — accepted inelastic background)

where $\Phi(t_0) = \Phi(E_0)\frac{dE_0}{dt_0} = \text{const} \times \Phi(E_0) \times E_0^{3/2}$, $\Phi(E_0)$ being the energy distribution of neutrons emerging from the moderator. This distribution is well described by the Maxwell function $\Phi(E_0) = E_0 \exp(-E_0/E_{\max})$ with $E_{\max} = 28.0$ meV.

The spectra presented in Fig. 3 (after being divided by the flux $\Phi(t_0)$ and normalized to the same height) are shown again in Fig. 4. The background under the quasi-elastic peak is mainly due to multiple and inelastic neutron scattering on the sample, and increases with sample temperature and scattering angle ϑ. This background is proportional to the intensity of neutrons incident to the sample and after being normalized by $\Phi(t_0)$ should have a constant value. Since our system of analysing the scattered neutron energy includes a beryllium filter, the transmission of which rises abruptly for neutrons of energies $E_0 < 5.24$ meV, the background for neutrons in this energy range is higher. Therefore, the step function depicted in Fig. 4 by the dashed line was accepted as the background.

After background subtraction the experimental spectrum was analyzed according to Eq. (4) as the convolution of the cross section described by the scattering law (1) with the spectrometer resolution function $R(E_f)$.

5. Fitting procedure and discussion of results

The spectrometer resolution was assumed to be the same as that presented by the shape of the peak measured for TBN's phase III, which may be said to be the outcome of pure elastic incoherent neutron scattering. In this case the cross section at a given angle and at a constant temperature of the sample can be written as

$$\sigma_{el}^{inc}(E_0, E_f, \vartheta, T) = \text{const} \times \delta(E_0 - E_f),$$

and on the basis of Eq. (4) we get $I^{III}(E_0) = R(E_0)$. Since the experimental values of the spectrum $I^{III}(E_0)$ are burdened by statistical spread and correspond only to some definite values of energy, the resolution was assumed to be in the form of an analytical function fitted to these values. This function is made up of two Gaussian functions

$$R(E) = \begin{cases} A_1 \exp[-B_1(E-E_0')^2], & E \leqslant E_c \\ A_2 \exp[-B_2(E-E_0'')^2], & E > E_c \end{cases} \tag{5}$$

In Fig. 5 the solid line depicts the shape of function (5) after the parameters A_1, A_2, B_1, B_2, E_0', E_0'' and E_c are fitted to the experimental points.

The shape of the quasi-elastic peak for TBN's phase II was analysed with the assumption that the cross section in this case can be described by the scattering law $S_{qns}^{inc}(\kappa, \omega)$ presented in Sec. 2 of this paper,

$$\sigma_{qns}^{inc}(E_0, E_f, \vartheta, T) = \frac{k_f}{k_0} \exp(-\hbar\omega/2k_BT) \times S_{qns}^{inc}(\kappa, \omega). \tag{6}$$

After Eqs (1) and (4) are taken into account and assuming a mean rotation radius r for all protons in the molecule we get

$$I^{II}(E_0) = \text{const}\left\{\frac{\pi}{2} F_{el}[\kappa(E_0)r] \times R(E_0)\right.$$

$$\left. + \int_{E_1}^{E_2} \sqrt{\frac{E_f}{E_0}} \exp\left(\frac{E_f - E_0}{2k_B T}\right) R(E_f) \sum_{l=1}^{n} F_{qel}^{(l)}[\kappa(E_0)r] \frac{\Gamma_l dE_f}{\Gamma_l^2 + (E_0 - E_f)^2}\right\}. \quad (7)$$

Here the parameters of the fit are the normalization constant "const" and the half-width of the first Lorentz function Γ_1. The limits of integration $E_1 = 4.3$ meV and $E_2 = 5.4$ meV define the energy range in which the resolution function is greater than zero. The fit of the

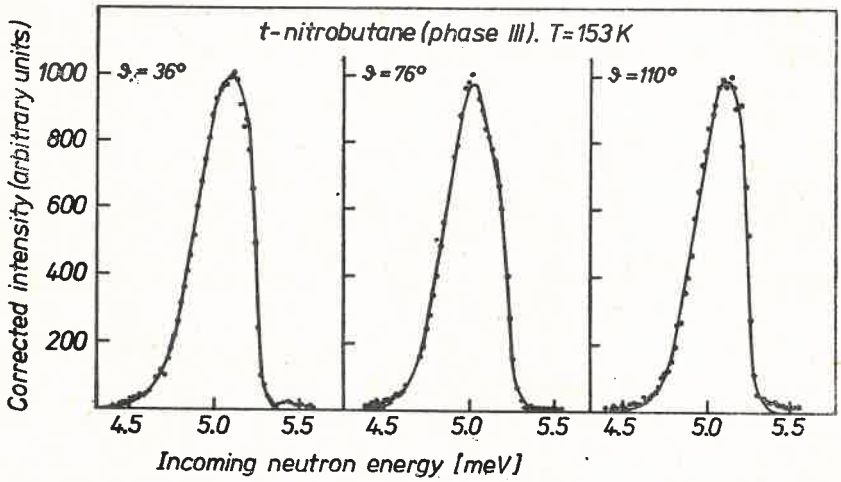

Fig. 5. Resolution functions of the spectrometer (solid lines correspond to two Gaussian functions)

parameters to the experimental data was accomplished with the use of the MINUITS program of the CERN Program Library [14] on the CYBER-72 computer of the CYFRONET Computing Center in Cracow.

The fundamental problem which should be solved first, when analyzing the experimental results obtained for phase II of TBN, is associating the observed quasielastic broadening with the character of the motion of protons in this phase. As has already been mentioned, we should consider the possibility of rotational jumps of the CH_3 groups around the C_3 axis ($r = 0.964$ Å) and the reorientation of the trimethyls around the C-N axis. Then as earlier for TBC [6] the rotation radius was assumed to be $r = 1.81$ Å, which corresponds to the radius over which the center of gravity of the CH_3 group's proton move in the rotation of the molecule around the C–X axis.

The results of the best fit of the model incorporating 120° jumps of the CH_3 groups

for each scattering angle are arranged in Table I. The quality of the fit is characterized by the parameter

$$\chi^2 = \frac{1}{N-NP}\sum_{i=1}^{N}\left[\frac{I_i^{\mathrm{exp}}(E_0)-I_i^{\mathrm{th}}(E_0)}{\Delta I_i^{\mathrm{exp}}(E_0)}\right]^2, \tag{8}$$

TABLE I

Values of Γ and χ^2 for 120°-jumps of CH_3 groups in Phase II of t-nitrobutane fitted to QNS data at different scattering angles

Scattering angle	$\varkappa$ [Å^{-1}] average momentum transfer	$\varkappa r$ (r = 0.964 Å)	Γ [meV] best fitted parameter	χ^2
36°	0.966	0.931	0.339	26.369
56°	1.467	1.414	0.306	10.738
76°	1.924	1.855	0.221	2.979
90°	2.210	2.130	0.184	4.419
110°	2.563	2.470	0.192	2.139
average value			0.248	9.329

where I^{exp} is the experimental intensity, I^{th} is the theoretical intensity according to Eq. (7), ΔI^{exp} is the error of the experimental value, N is the number of measured points, and $NP = 2$ is the number of fitted parameters. When the model gives a good fit, the parameter χ^2 should be near unity. As seen from Table I, the model of 120°-jumps of CH_3 groups cannot explain the quasi-elastic broadening observed for the low scattering angles of 36° and 56°. Such a result should have been expected because for these angles the observed share of the quasi-elastic scattering is much greater than follows from the form factor ratio for $\varkappa r = 0.93$ (Fig. 2). It can be assumed, therefore, that this broadening is associated with a much greater radius of proton rotation, hence, with the rotation of the trimethyls around the C-N axis of TBN molecule.

TABLE II

Parameters fitted to QNS data and χ^2 for two models of uniaxial reorientation of t-nitrobutane molecule

ϑ scattering angle	$\varkappa r$ (r = 1.81 Å)	120°-jumps		Uniaxial rotational dif.	
		Γ [meV] best fitted parameter	χ^2	Γ_1 [meV] best fitted parameter	χ^2
36°	1.748	0.181	3.808	0.1615	4.349
56°	2.656	0.147	1.638	0.0866	1.554
76°	3.483	0.186	2.555	0.0503	2.495
90°	4.000	0.274	3.724	0.0314	3.929
110°	4.638	0.304	4.225	0.0289	2.644
average value		0.218	3.190	0.0717	2.994

The second step in the analysis of the data was to obtain the best fitted parameters for the 120°-jump model and the model of uniaxial rotational diffusion of the trimethyls for each scattering angle. A comparison of the fits obtained is given in Table II. The χ^2 test in the fitting of a free model parameter independently for each scattering angle does not give preference to any of these models. However, for the rotational diffusion model there is a pronounced systematic change of Γ_1 depending on κr, which should not occur. For the fitted half-width of the Lorentz function Γ gives a time characteristics of the proton motion and is a function of the sample temperature but not of the scattering angle. The

TABLE III

χ^2 value for the model of 120°-jumps of t-nitrobutane molecule at Γ = const for all scattering angles

Scattering angle	$\Gamma = 0.1$ meV	$\Gamma = 0.15$ meV	$\Gamma = 0.2$ meV	$\Gamma = 0.25$ meV	$\Gamma = 0.3$ meV
36°	10.02	4.54	4.01	6.12	9.55
56°	4.81	1.65	4.33	9.83	16.47
76°	10.86	3.74	2.71	5.18	9.51
90°	13.12	7.54	4.83	3.82	3.82
110°	11.65	7.67	5.52	4.51	4.23
$\frac{1}{5}\sum_{i=1}^{5}\chi^2$	10.09	5.029	4.280	5.892	8.723

geometry of the proton motion is incorporated in the neutron scattering law (Eq. (1)) only through the form factors $F_{el}(\kappa r)$ and $F_{qel}(\kappa r)$. The next step (in the analysis) was, to test χ^2 at a fixed value of the model parameter for all scattering angles. The results of calculations for the 120°-jump models are arranged in Table III, while Fig. 6 shows the

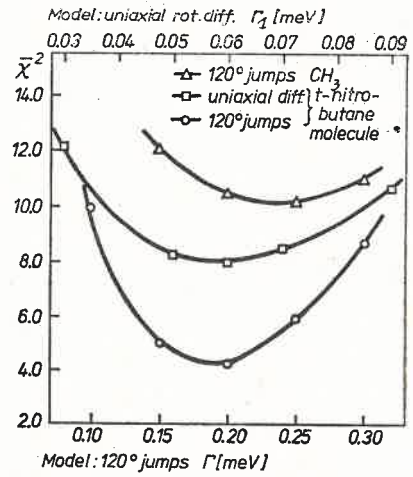

Fig. 6. χ^2 test for three models of proton rotation in TBN's phase II

mean values $\bar{\chi}^2 = \frac{1}{5}\sum_{i=1}^{5}\chi^2$ obtained for all of the three proton motion models discussed in this paper.

A comparison of the shapes of the peaks calculated from Eq. (7) with experimental data for values of the parameter corresponding to minimum $\bar{\chi}^2$ (for the various models) is given in Fig. 7. Figure 7A depicts the situation for a model of 120°-jumps of both CH_3

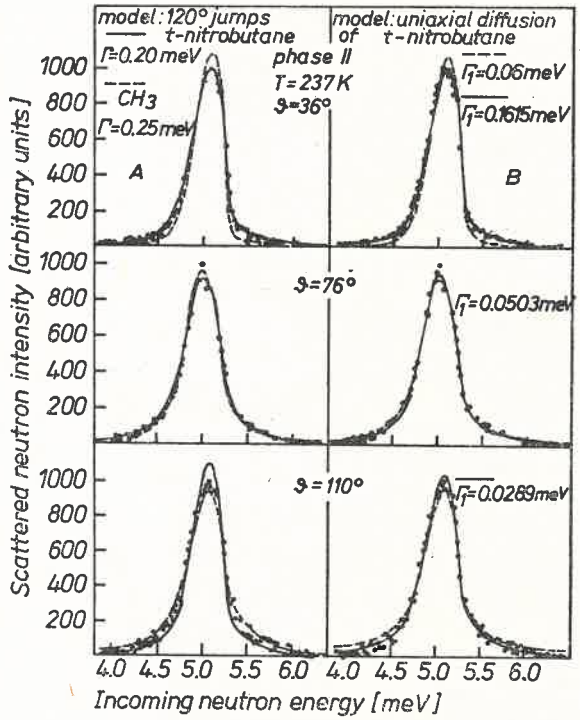

Fig. 7. Comparison of experimental intensities with theoretical curves based on two models of TBN's molecule rotation in phase II

and trimethyl groups. As can be seen, the model of trimethyl rotation renders the quasi-elastic peak shape well for small ϑ angles, but worse for large angles.

It follows from Table III and Figs 6 and 7 that none of the one-parameter models of stochastic reorientation of protons in TBN's phase II explain the observed quasi-elastic broadening of scattered neutron peaks with sufficient accuracy. It seems that a better description of the shape of the observed peaks would be obtained if both models of proton motion were considered simultaneously. Due to the low spectrometer resolution, the quality of this experiment is not good enough for fitting multi-parameter models. This is to a certain extent, illustrated by Fig. 7B, in which the solid line depicts the fit of the model of uniaxial rotational diffusion of the trimethyl with the model parameter varying with each scattering angle. Then there is good agreement of the thereotical curve with the points measured. However, once the Γ_1 parameter is established (its value corresponds

to minimum $\bar{\chi}^2$) the deviation of the curve from the points becomes more evident (the dashed line in Fig. 7B). Hence, Fig. 7 shows how important the extent of the range of momentum transfers and the degree of the energy resolution in the QNS experiment are when verifying the correctness of an assumed model of molecule reorientation in a crystal.

Assuming that the model of 120°-jumps of trimethyls depicts the dynamic situation of the TBN molecules in phase II best, it is possible to find the mean time a molecule spends in the potential well on the basis of the determined Lorentz curve half-width. This amount to $\tau = \frac{3}{2} \times \frac{h}{\Gamma} = (3.1 \pm 0.3) \times 10^{-11}$ sec, which corresponds to a jump frequency $\nu_{\text{jump}} = 3.22 \times 10^{10}$ sec^{-1} (at $T = 237$ K).

Interpreting the qns broadening observed in the spherical harmonics formalism [15, 16] we get the values of correlation times for the model of 120°-jumps of trimethyls

$$\tau_1 = \tau_2 = \ldots = \tau_l = \hbar/2\Gamma = (1.65 \pm 0.1) \times 10^{-12} \text{ sec},$$

whereas for the rotational diffusion model

$$\tau_1 = \hbar/2\Gamma_1 = (5.5 \pm 0.5) \times 10^{-12} \text{ sec},$$

$$\tau_2 = \hbar/2\Gamma_2 = (1.4 \pm 0.1) \times 10^{-12} \text{ sec}.$$

Although the results of the analysis of the QNS experiment give preference rather to the trimethyl 120°-jump model, it would be enlightening to have an experiment which allows the time τ_1 to be determined (dielectric relaxation, IR), as its value depends heavily on the assumed rotation model.

6. Conclusions

The analysis performed on the results of the QNS experiment for TBN allows the following conclusions to be drawn:

1. In phase II of TBN there are rapid stochastic reorientation movements of protons, which vanish after the transition to phase III.

2. The one-parameter models of 120°-jumps of protons and uniaxial rotational diffusion cannot satisfactorily explain the observed shape of QNS peaks in the examined range of neutron momentum transfers. However, the results of the analysis imply that:

— the radius of proton rotations is large which supports the idea of the whole molecule rotating around the C-N bond, and

— there are rather large angular jumps of the molecules, probably by angles of the order of 120°, with a correlation time of about 1.6 psec.

3. The approximation of real stochastic motions of molecules in substances of the $(CH_3)_3CX$ type by the one-parameter model is too rough even for phases in which the C–*X* bond is frozen [6]. A better fit of theoretical curves to experimental patterns could be achieved by considering many-parameter models which account for:

— the duration of the proton jumps from one equilibrium state to another,

— jumps of both molecules and CH_3 groups,

— combinations of jumps with the diffusive motion of molecules,

— combinations of molecule jumps by various angles.

4. Verification of many-parameter models of stochastic uniaxial reorientation of protons requires performing a QNS experiment with much better resolution, so that the shape of the analysed peak would better reproduce the shape of the measured scattering law. Moreover in order to provide coverage for a large interval of κr values an experiment like this should comprise the broadest range of neutron momentum transfers possible.

The authors wish to express their appreciation to Professor J. A. Janik and Dr W. Nawrocik for invaluable comments and discussions in the processing of the results, and to Dr M. Sudnik-Hrynkiewicz and S. I. Bragin for assistance in performing the measurements.

REFERENCES

[1] S. Urban, Z. Tomkowicz, J. Mayer, T. Waluga, *Acta Phys. Pol.* **A48**, 61 (1975).
[2] S. Urban, *Acta Phys. Pol.* **A49**, 741 (1976).
[3] P. Freundlich, J. Kalenik, E. Narewski, L. Sobczyk, *Acta Phys. Pol.* **A48**, 701 (1975).
[4] S. Urban, J. Domosławski, Z. Tomkowicz, (to be published).
[5] R. Haffmans, I. W. Larkin, *J. Chem. Soc. Faraday Trans. II* **68**, 1729 (1972).
[6] P. S. Goyal, W. Nawrocik, S. Urban, J. Domosławski, I. Natkaniec, *Acta Phys. Pol.* **A46**, 399 (1974).
[7] R. Rudman, B. Post, *Molecular Crystals* **5**, 95 (1968).
[8] T. Springer, Springer Tracts in Modern Physics, Vol. 64, Springer-Verlag, Berlin 1972.
[9] P. S. Goyal, I. Natkaniec, W. Nawrocik, J. Domosławski, Report No E14-7648, JINR Dubna (1973).
[10] K. Sköld, *J. Chem. Phys.* **49**, 2443 (1968).
[11] J. A. Janik, J. M. Janik, K. Otnes, K. Rościszewski, *Physica* **83B**, 259 (1976).
[12] K. Parliński, M. Sudnik-Hrynkiewicz, A. Bajorek, J. A. Janik, W. Olejarczyk, *Research Applications of Nuclear Pulsed Systems*, IAEA, p. 179 (1967), Vienna, Report No 727/E of the Institute of Nuclear Physics, Cracow 1966.
[13] M. Sudnik-Hrynkiewicz, W. Olejarczyk, R. Zieleniewski, A. Szkatuła, J. A. Janik, A. Bajorek, *Nukleonika* **12**, 385 (1967).
[14] F. James, M. Ross, Program MINUITS, CERN Computer Library.
[15] V. F. Sears, *Can. J. Phys.* **44**, 1299 (1966).
[16] C. Brot, B. Lassier-Govers, *Ber. Bunsenges. Phys. Chem.* **80**, 31 (1976).